Available online at www.sciencedirect.com
ScienceDirect
Dyes and Pigments 78 (2008) 165–172
DYES and PIGMENTS
www.elsevier.com/locate/dyepig

Amino-containing saturated red light-emitting copolymers based on fluorene and carbazole units

Rong Guan, Chun Li, Wei Yang*, Wenbin Sun, Hongbin Wu, Lei Ying, Yong Cao

Institute of Polymer Optoelectronic Materials and Devices, Key Lab of Specially Functional Materials, Ministry of Education, South China University of Technology, Guangzhou 510640, China

Received 3 August 2007; received in revised form 21 November 2007; accepted 21 November 2007
Available online 8 December 2007

Abstract

Amino-containing copolymers were synthesized by Suzuki polycondensation based on 9,9-di(2-ethylhexy)fluorene, 9-dimethylaminopropyl carbazole and 4,7-di(4-hexyl-2-thienyl)-2,1,3-benzothiadiazole (≤15 mol%) units. The copolymers had high glass-transition temperature (T_gs: 86–145 °C), excellent thermal stability ($T_{d\ (5\%\ loss)}$: 400 °C) and emitted red light at 658 nm. The peak was shifted from 614 to 658 nm when the 4,7-di(4-hexyl-2-thienyl)-2,1,3-benzothiadiazole content was increased from 0.1 to 15 mol%. The dimethylaminopropyl group in the side chain of the copolymer significantly lowered the barrier height of the interface between the metal cathode and the polymer. Thus, aluminium can be used as the cathode in polymer light-emitting devices and operated at a level of performance similar to that achieved with metal cathodes such as barium.

Keywords: Fluorene; Amino-containing carbazole; Copolymers; Red emission; Al cathode

1. Introduction

Polymer light-emitting devices (PLEDs) have received remarkable scientific and industrial attentions due to their potential applications in large area flat-panel displays [1–3]. During the past decades, a variety of conjugated polymers have been synthesized in order to identify promising candidates for high-resolution, full color, flat-panel displays [4–6].

Polyfluorenes (PFs) and their derivatives have emerged as a promising class of light-emitting conjugated polymers because of their high photoluminescent (PL) and electroluminescent (EL) yields as well as easy tenability of physical properties through chemical structure modification and/or copolymerization [7–9]. The emission color of polyfluorenes also can be tuned over entire visible region by incorporating narrow-band gap co-monomers into polyfluorene backbone [10–12]. Red light-emitting polyfluorene was first synthesized by alternating copolymerization of fluorene and 4,7-dithienyl-2,1,3-benzothiadiazole (DBT) [13], after which, a series of saturated red-emitting copolymers were synthesized by using different co-monomers such as qunquethithiphene-1″,1″-dioxide [14,15], 2,5-bis(2′-vinyl-thienyl) thiophene [16], and 2,1,3-naphthoselenadiazole [17].

It is well known that good electron and hole injections are necessary to obtain highly efficient PLEDs [18,19]. Recently, Huang et al. reported the amino-containing polyfluorene-based conjugated polymers with a small amount of narrow-band gap (NBG) co-monomers such as 2,1,3-benzothiazole [20] in the polymer main chain, and found that these kinds of polymers could provide good device performance by using a high-work-function metal such as Al, Ag, Au as the cathode, due to interface dipole formation between the light-emitting polymer and the high-work-function cathode [21].

Carbazole-based copolymers have good hole-injection properties due to the electron-donating capabilities associated with the nitrogen in carbazole unit [22–27]. Therefore, the

* Corresponding author. Fax: +86 20 87110606.
E-mail address: pswyang@scut.edu.cn (W. Yang).

0143-7208/$ - see front matter © 2007 Elsevier Ltd. All rights reserved.
doi:10.1016/j.dyepig.2007.11.007

incorporation of carbazole unit into the polymer chain will effectively raise the highest occupied molecular orbital (HOMO) energy levels and reduce the barrier height for hole injection between the anode or anode buffer layer and the light-emitting layer in PLEDs.

In this paper, with the purpose of utilizing high-work-function metal as cathode and more effectively reducing the barrier height for hole injection, aminoalkyl group containing carbazole unit was employed since it can facilitate electron and hole injection simultaneously. The copolymers based on fluorene, containing aminoalkyl group carbazole (CzN) and 4,7-di(4-hexyl-2-thienyl)-2,1,3-benzothiadiazole (DHTBT) units were synthesized and investigated.

2. Experimental part

2.1. Materials

All reagents, unless otherwise specified, were purchased from Aldrich and Acros, and were used as received. All solvents were carefully dried and purified under nitrogen flow. All manipulations involving air-sensitive reagents were performed in a dry argon atmosphere. The monomer 2,7-bis(4,4,5,5-tetramethyl-1,3,2-dioxaborolan-2-yl)-9,9-di(2-ethylhexyl)-fluorene (**1**) was synthesized according to published procedure [28].

2.2. Instrumentations

The ^{1}H and ^{13}C NMR spectra were recorded on a Bruker DRX 300 in deuterated chloroform solution. The number-average molecular weights (M_n) were determined by a Waters GPC 2410 in tetrahydrofuran (THF) with a calibration curve of polystyrene standards. Elemental analyses were performed on a Vario EL elemental analysis instrument (Elementar Co.). UV–vis absorption spectra were recorded on an HP 8453 UV–vis spectrophotometer. Cyclic voltammetry was carried out on a CHI660A electrochemical workstation in a solution of tetrabutylammonium hexafluorophosphate (Bu_4NPF_6, 0.1 M) in acetonitrile (CH_3CN) at a scanning rate of 50 mV/s at room temperature under argon. A platinum electrode coated with a thin polymer film was used as the working electrode. A Pt plate was used as the counter electrode and a saturated calomel electrode was used as the reference electrode. The thermogravimetric analysis (TGA) of the polymers was performed at a heating rate of 20 °C/min with a NETZSCH TGA-209 thermal analyzer under nitrogen atmosphere. The thermal transitional properties of the polymers were measured with a NETZSCH DSC-204 differential scanning calorimeter (DSC) under a nitrogen atmosphere at a heating rate of 10 °C/min.

The photoluminescence (PL) efficiencies were determined in an IS080 integrating sphere (Labsphere) with 325 nm excitation of a HeCd laser (Mells Griot). PL and EL spectra were recorded on an Instaspec IV CCD spectrophotometer (Oriel Co.).

2.3. Synthesis of 3,6-dibromo-9-dimethylamiopropylcarbazole (**2**)

3,6-Dibromocarbazole (9.75 g, 30 mmol), NaH (0.96 g, 40 mmol) and 100 mL THF were added to a three-necked flask and stirred at room temperature for 2 h under a nitrogen atmosphere. 3-Dimethylaminopropyl chloride hydrochloride (11.0 g, 70 mmol) and NaOH (3.0 g, 75 mmol) were first diluted in 20 mL water and cooled, then the upper layer of solution was added dropwise to the above mixture. The reaction mixture was refluxed for an additional 24 h. After the removal of the solvent under a reduced pressure, the residue was purified by column chromatography on silica gel using petroleum ether/ethyl acetate/triethylamine (v/v = 20:5:1) as eluent. Recrystallization from ethanol gave the compound (yield: 88%) as white solid, mp: 118–119 °C. ^{1}H NMR (300 MHz, $CDCl_3$) δ (ppm): 8.12 (d, $J = 1.89$ Hz, 2H), 7.54 (dd, $J_1 = 1.89$ Hz, $J_2 = 8.70$ Hz, 2H), 7.35 (d, $J = 8.70$ Hz, 2H) (carbazole ring), 4.33 (t, $J = 6.66$ Hz, 2H, carbazole–N–CH_2–), 2.20 (s, 6H, –N–CH_3), 2.18 (t, $J = 3.72$ Hz, 2H, –N–CH_2–), 1.97 (m, 2H, –CH_2–). ^{13}C NMR (75 MHz, $CDCl_3$) δ (ppm): 139.44, 129.01, 123.45, 123.18, 112.00, 110.61 (carbazole rings), 56.14 (carbazole–N–CH_2–), 45.39 (–N–CH_2–), 40.70 (–N–CH_3), 26.79 (alkyl, –CH_2–). Element Anal. Calcd for $C_{17}H_{18}Br_2N_2$: C, 49.78%; H, 4.42%; N, 6.83%. Found: C, 49.80%; H, 4.46%; N, 6.80%.

2.4. Synthesis of 4,7-bis(5-bromo-4-hexyl-2-thienyl)-2,1,3-benzothiadiazole (**3**) [29–31]

To a solution of 3-hexylthiophene in anhydrous THF at −30 °C, *n*-BuLi was added dropwise and the mixture was stirred at the same temperature under N_2 for 2 h. Then tributylchlorostannane was added, and the mixture was stirred at −30 °C for 30 min. The mixture was poured into saturated aqueous sodium hydrogen carbonate, and the organic phase was separated and washed with saturated aqueous brine and then dried over an anhydrous sodium sulfate. The solvent was removed under a reduced pressure, and the residue was purified by column chromatography on neutral alumina using petroleum ether as eluent to give tributyl-(4-hexyl-2-thienyl)stannane as colorless oil. The $PdCl_2(PPh_3)_2$ was added to a solution of 4,7-dibromo-2,1,3-benzothiadiazole and tributyl-(4-hexyl-2-thienyl)stannane in THF. The mixture was refluxed in a nitrogen atmosphere for 6 h. After the removal of the solvent, the residue was purified by column chromatography on silica gel using petroleum ether/dichloromethane (v/v = 1:1) as eluent. Recrystallization from ethanol gave the compound 4,7-di(4-hexyl-2-thienyl)-2,1,3-benzothiadiazole as orange needles, which were dissolved into THF solution. After the solid dissolved completely, *N*-bromosuccinimide (NBS) was added in one portion. The mixture was stirred at a room temperature for 2 h, then the hexane was added into the mixture. The white precipitate formed was filtered off and the filtrate was extracted with ether. The organic phase were combined and washed with brine and dried over anhydrous sodium sulfate. The solvent was removed at a reduced pressure to give the

product as a red solid (yield: 82%), mp: 102–103 °C. ^{1}H NMR (300 MHz, $CDCl_3$) δ (ppm): 7.75 (s, 2H, benzothiadiazole ring), 7.70 (s, 2H, thiophene rings), 2.63 (t, $J = 7.50$ Hz, 4H, $-CH_2-$), 1.71–1.62 (m, 4H, $-CH_2-$), 1.43–1.25 (m, 12H, $-CH_2-$), 0.93–0.89 (m, 6H, $-CH_3$). ^{13}C NMR (75 MHz, DCl_3) δ (ppm): 152.20, 143.07, 138.49, 128.06, 125.27, 124.81, 111.62 (aryl rings), 31.66, 29.76, 29.70, 28.99, 22.64, 14.13 (alkyl chain). Element Anal. Calcd for $C_{26}H_{30}N_2S_3Br_2$: C, 49.84%; H, 4.83%; N, 4.47%; S, 15.35%. Found: C, 50.58%; H, 5.06%; N, 4.37%; S, 14.86%.

3. Polymerization

General procedures of Suzuki polycondensation taking PFCzN–DHTBT1 as an example: 2,7-bis(4,4,5,5-tetramethyl -1,3,2-dioxaborolan-2-yl)-9,9-di(2-ethylhexyl)-fluorene (**1**) (0.642 g, 1 mmol), 3,6-dibromo-9-dimethylaminopropylcarbazole (**2**) (0.4018 g, 0.98 mmol), 4,7-bis(5-bromo-4-hexyl-2-thienyl)-2,1,3-benzothiadiazole (**3**) (0.0125 g, 0.02 mmol), and $(PPh_3)_4Pd(0)$ (8 mg) were dissolved in 10 mL mixture of toluene/THF (2:1(v/v)) and 2 mL of 2 M Na_2CO_3 aqueous solution. The mixture was refluxed with vigorous stirring for 3 days under argon. Then 2-(4,4,5,5-tetramethyl-1,3,2-dioxaborolan-2-yl)-9,9-di(2-ethylhexyl)fluorene (0.064 g) and bromobenzene(0.4 mL) were added and continue reaction for 12 h, respectively. The whole mixture was poured into methanol. The resulted solid was filtered and washed for 24 h with mixture solution acetone/water to remove oligomers and catalyst residues. Yield: 70%.

PFCzN–DHTBT1: ^{1}H NMR (300 MHz, $CDCl_3$) δ (ppm): 8.44 (s, 2H), 7.85–7.72 (m, 8H), 7.60–7.57 (m, 2H) (aryl rings), 4.49 (br s, 2H, carbazole–N–CH_2-), 2.38–2.16 (m, 16H), 0.94–0.59 (m, 35H) (alkyl chain). Element Anal. Found: C, 84.36%; H, 9.01%; N, 3.78%; S, 0.43%.

PFCzN–DHTBT5: ^{1}H NMR (300 MHz, $CDCl_3$) δ (ppm): 8.44 (s, 2H), 7.85–7.71 (m, 8H), 7.60–7.57 (m, 2H) (aryl rings), 4.49 (br s, 2H, carbazole–N–CH_2-), 2.83–2.71 (m, 1H), 2.37–2.29 (m, 14H), 1.68 (m, 2H), 1.33 (m, 2H), 0.93–0.61 (m, 36H) (alkyl chain). Element Anal. Found: C, 84.92%; H, 8.72%; N, 3.36%; S, 1.57%.

PFCzN–DHTBT10: ^{1}H NMR (300 MHz, $CDCl_3$) δ (ppm): 8.44 (s, 2H), 7.85–7.72 (m, 8H), 7.60–7.57 (m, 2H) (aryl rings), 4.49 (br s, 2H, carbazole–N–CH_2-), 2.82–2.72 (m, 1H), 2.37–2.16 (m, 16H), 1.74 (m, 2H), 1.34 (m, 4H), 0.93–0.59 (m, 44H) (alkyl chain). Element Anal. Found: C, 83.02%; H, 9.15%; N, 3.86%; S, 2.59%.

PFCzN–DHTBT15: ^{1}H NMR (300 MHz, $CDCl_3$) δ (ppm): 8.44 (s, 2H), 7.87–7.72 (m, 9H), 7.60–7.49 (m, 4H) (aryl rings), 4.49 (br s, 2H, carbazole–N–CH_2-), 2.83–2.71 (m, 1H), 2.37–2.13 (m, 15H), 1.74 (m, 2H), 1.38–1.26 (m, 5H), 0.93–0.55 (m, 46H) (alkyl chain). Element Anal. Found: C, 83.42%; H, 8.86%; N, 3.78%; S, 3.52%.

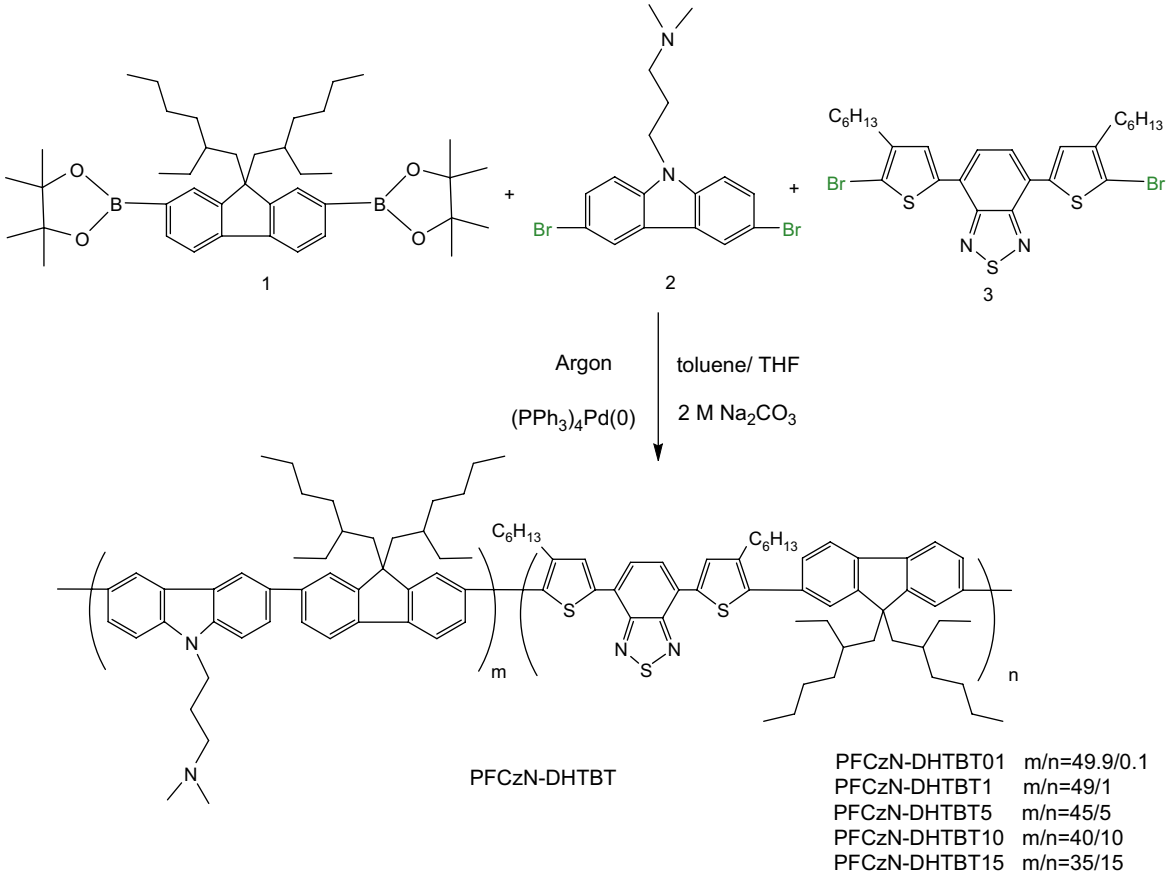

Scheme 1. Synthetic routes for copolymers.

Table 1
Physical and thermal properties of the polymers

Polymer	M_n ($\times 10^3$)	PDI	DHTBT/CzN/F content (mol%)		T_g (°C)	T_d[b] (°C)
			In feed ratio	In polymer[a]		
PFCzN–DHTBT01	10.0	1.5	0.1/49.9/50	0.1/49.6/50.3	145	395
PFCzN–DHTBT1	6.6	1.6	1/49/50	1.5/48.4/50.1	141	400
PFCzN–DHTBT5	8.4	1.3	5/45/50	5.1/44.7/50.2	100	403
PFCzN–DHTBT10	9.3	1.3	10/40/50	9.7/39.8/50.5	97	412
PFCzN–DHTBT15	6.4	1.4	15/35/50	14/36/50	86	404

[a] Calculated from the results of elemental analysis.
[b] Temperature at a 5% weight loss.

3.1. LED fabrication and characterization

The PLEDs were fabricated on ITO-covered glass substrates. Patterned indium tin oxide (ITO)-coated glass substrates were cleaned with acetone, detergent, distilled water, and isopropyl alcohol, subsequently in an ultrasonic bath. After treatment with oxygen plasma, 150 nm of poly(3,4-ethylenedioxythiophene) (PEDOT) doped with poly(styrenesulfonic acid) (PSS) (Batron-P 4083, Bayer AG) was spin-coated onto the ITO substrate followed by drying in a vacuum oven at 80 °C for 8 h. For some devices, poly(vinylcarbazole) (PVK, Aldrich) from 1,1,2,2-tetrachloroethane solution was coated on top of a dried PEDOT–PSS layer subsequently. The polymers were dissolved in toluene and filtered through a 0.45 μm filter. A thin film of polymer was coated onto the anode by spin-casting inside a dry box. The film thickness of the active layers was around 70 nm, as measured with an Alfa Step 500 surface profiler (Tencor). A thin layer of Ba (4–5 nm) and subsequently Al (200 nm) were vacuum-evaporated subsequently on the top of the EL polymer layer under a vacuum of 1×10^{-4} Pa. Device performances were measured inside a dry-box. Current–voltage (I–V) characteristics were recorded by a Keithley 236 source meter. EL spectra were recorded by Oriel Instaspec IV CCD spectrograph. Luminance was measured by a PR 705 photometer (Photo Research). The external quantum efficiencies were determined by a Si photodiode with calibration in an integrating sphere (IS080, Labsphere).

To avoid contamination of volatile low-work-function metal (Ba) during Al cathode deposition on top of the PFCzN–DHTBT layer, an evaporation chamber was thoroughly cleaned through baking at 120–130 °C and at a high vacuum ($<1 \times 10^{-4}$ Pa) before Al deposition. The control devices [ITO/PEDOT/MEH–PPV/(or Ba)Al] were fabricated. The extra quantum efficiencies of the devices 1.94% and 0.014%, respectively, with the configuration: ITO/PEDOT/MEH–PPV/(or Ba)/Al ensured that high-work-function metal Al was not contaminated by low-work-function Ba in the evaporation chamber from the previous deposition.

4. Results and discussion

4.1. Synthesis and characterization

Copolymers were synthesized from co-monomers **1**, **2** and **3** by Suzuki polycondensation (shown in Scheme 1). The feed ratios of DHTBT monomer are 0.1, 1, 5, 10, 15 mol%, and the corresponding copolymers are named, respectively, as PFCzN–DHTBT01, PFCzN–DHTBT1, PFCzN–DHTBT5, PFCzN–DHTBT10 and PFCzN–DHTBT15. The monomer feed molar ratios were adjusted in order to investigate the effect of composition on the physical and optical properties of copolymers. The actual composition of PFCzN–DHTBT copolymer calculated from the sulfur, nitrogen and carbon results of elemental analyses is close to the feed ratios of monomers as listed in Table 1. All the copolymers have good solubility in common solvents such as chloroform, toluene, and THF, since 2-ethylhexyl substituents in the 9-position of fluorene and *n*-hexyl substituents in the 4-position of thiophene and 9-dimethylaminopropyl group in the N-position of carbazole were employed to improve the solubility of the resulted copolymers. The number-average molecule weights (M_n) of the synthesized copolymers are in the range of 6000–10000 g/mol with polydispersity index (PDI) of around 1.3–1.6, typical for a polycondensation reaction.

The thermal properties of polymers were evaluated by TGA and DSC. TGA reveals excellent thermal stabilities of copolymers as shown in Fig. 1. The thermal decomposition temperatures (5% weight loss) of PFCzN–DHTBT01, PFCzN–DHTBT1, PFCzN–DHTBT5, PFCzN–DHTBT10 and PFCzN–DHTBT15 are 395, 400, 403, 412 and 404 °C,

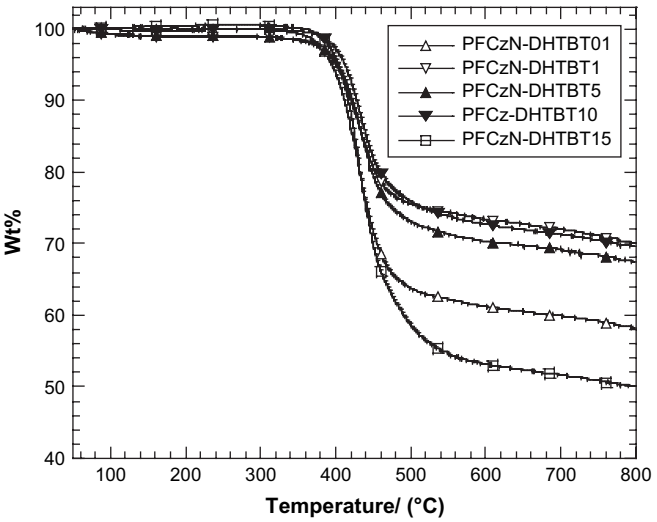

Fig. 1. TGA curves of the copolymers.

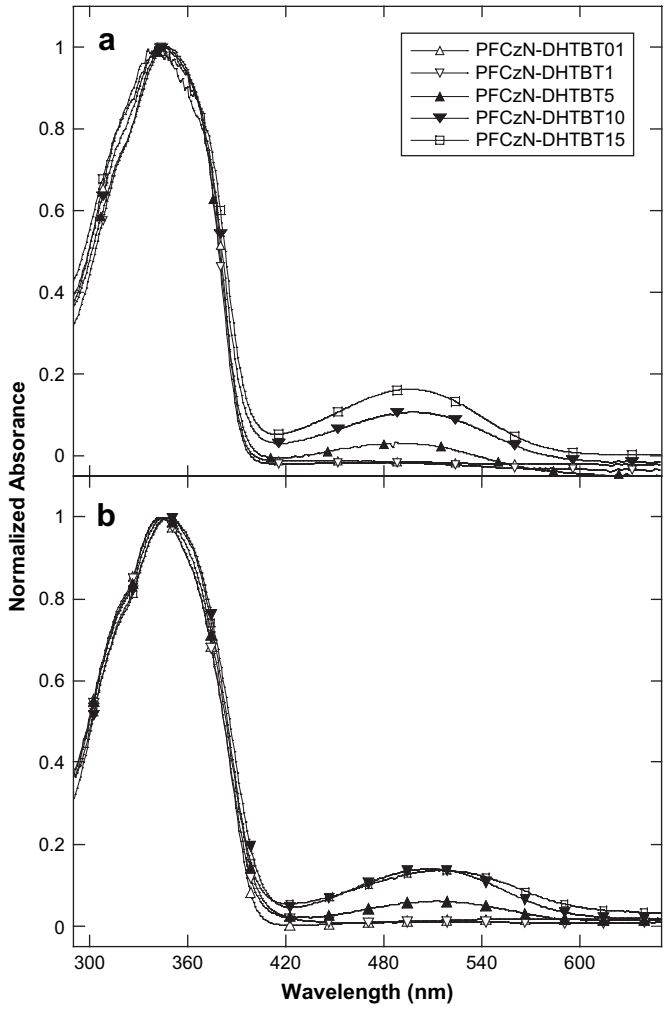

Fig. 2. UV–vis absorption spectra for the polymers: (a) in $CHCl_3$ (solution 10^{-4} mol/L) and (b) in film.

respectively (Table 1). The residual weights of copolymers are all greater than 50% when the temperature rise to 800 °C. The high residual yields of the copolymers could be explained by the intramolecular carbonization during the heating process due to their torsion structure in the backbone, which makes two nearby main chains carbonize easily with each other [32]. All the copolymers showed same one-step decomposition process and the initial weight loss started at about 350 °C, which could be ascribed to side chain decomposition upon heating process. The glass-transition temperature (T_g) of PFCzN–DHTBT01, PFCzN–DHTBT1, PFCzN–DHTBT5, PFCzN–DHTBT10 and PFCzN–DHTBT15 were 145, 141, 100, 97 and 86 °C (Table 1), as determined by differential scanning calorimetry (DSC). With the content of DHTBT unit increasing, the T_gs of the copolymers decrease. This owes to the weaker intermolecular interactions and the increasing intrachain irregularity caused by introducing more DHTBT units to copolymer main chain [33].

4.2. UV–vis absorption and electrochemical properties

The absorption spectra of the copolymers in $CHCl_3$ solution and in film are shown in Fig. 2. All the polymers show similar absorption spectra in solution (Fig. 1a) and in film (Fig. 1b). The spectra of copolymers are dominated by two absorption bands peaked at around 345 nm (Table 2), which can be attributed to the FCzN segments [32] in the copolymers, and peaked at around 510 nm, which can be attributed to the DHTBT unit incorporated into the polymer main chain [30]. The low-energy absorption intensities increase with the increasing content of DHTBT unit in the copolymers.

The electrochemical properties of the copolymers were investigated by cyclic voltammetry (CV) in order to gauge their electronic properties. All the electrochemical data of the copolymers obtained from the films are listed in Table 2. The copolymers show one p-doping wave but failed to detect n-doping process. The copolymers show only one quasi-reversible oxidation wave with the onsets around 0.83–0.87 eV. The oxidation waves can be assigned to the oxidation process for the PFCzN segment [32]. The highest occupied molecular orbital (HOMO) levels are calculated according to the following empirical formulas: $E_{HOMO} = -e(E_{ox} + 4.40)$ (eV) [34], and the lowest unoccupied molecular orbital (LUMO) levels are estimated from the optical band gap that are calculated from the absorption onset of copolymers in thin film (Table 2). HOMO and LUMO levels of copolymers, respectively, decrease from −5.23 and −2.13 eV to −5.27 and −3.19 eV with the increase of DHTBT content, indicating a much lower barrier for hole and electron injection from PEDOT–PSS (5.2 eV) [35], and Ba (2.8 eV) or Al (4.2 eV) [36], respectively.

Table 2
Optical and electrochemical properties of the copolymers

Polymer	λ_{abs} (nm)	Band gap[a] (eV)		E_{ox} (V)	HOMO (eV)	LUMO[b] (eV)	λ_{PL} (nm)	QE_{PL} (%)
		PFCzN	DHTBT					
PFCzN–DHTBT01	343	3.10	–	0.83	−5.23	−2.13	414, 595	49
PFCzN–DHTBT1	344	3.08	–	0.85	−5.25	−2.17	415, 613	67
PFCzN–DHTBT5	345, 507	3.05	2.11	0.84	−5.24	−3.13	415, 615	41
PFCzN–DHTBT10	347, 512	3.03	2.09	0.87	−5.27	−3.18	415, 634	41
PFCzN–DHTBT15	347, 515	3.04	2.08	0.87	−5.27	−3.19	415, 636	36

[a] Estimated from the onset wavelength of absorption of polymers in film.
[b] Calculated from HOMO level and the optical band gap.

4.3. Photoluminescence properties

Fig. 3 shows the PL spectra of the copolymers in $CHCl_3$ solution and in the thin film, respectively. In $CHCl_3$ solution (Fig. 3a), with the copolymer concentration of 1×10^{-5} mol/L (by repeat unit), except copolymer PFCzN–BHTBT01, all the copolymers show two emission peaks at around 405 and 630 nm. The emission intensities peaked at 405 nm decrease while the intensities peaked at 630 nm increase with increasing the DHTBT content in the copolymers. Therefore, 405 and 630 nm emissions can be assigned to FCzN segment and DHTBT unit in the copolymers, respectively. In the thin film, the emission of FCzN segment is completely quenched except the copolymer PFCzN–BHTBT01, and PL emission is dominated by the red emission at around 630 nm with the DHTBT content even as low as 1 mol% (Fig. 3b). PL emission peaks are gradually red-shifted with the increasing DHTBT content in the copolymers, from 595 nm for PFCzN–BHTBT01 to 636 nm for PFCzN–BHTBT15. The PL efficiencies (QE_{PL}) of the copolymers are listed in Table 2. All the polymers possess high PL efficiencies due to the effective intra- and intermolecular energy transfer in these copolymers. It is shown that the PL efficiencies increase when small amount of DHTBT unit are introduced into polymer backbone. The PL efficiencies of PFCzN–DHTBT01 and PFCzN–DHTBT1 are enhanced up to 49% and 67%, respectively, compared with 19% for PF-*alt*-CzN copolymer [32]. Further increasing DHTBT content to 15 mol%, the PL efficiencies of copolymers are slightly decreased from 41% for PFCzN–DHTBT5 to 36% for PFCzN–DHTBT15. It is due to the fact that the strong inter-chain interaction between amino-alkyl-substituted cabarzole unit is disturbed severely by the small amount of DHTBT unit introduced into polymer backbone, which suppress both radiative decay from FCzN segment and excimer emission in PFCzN inter-chain aggregates.

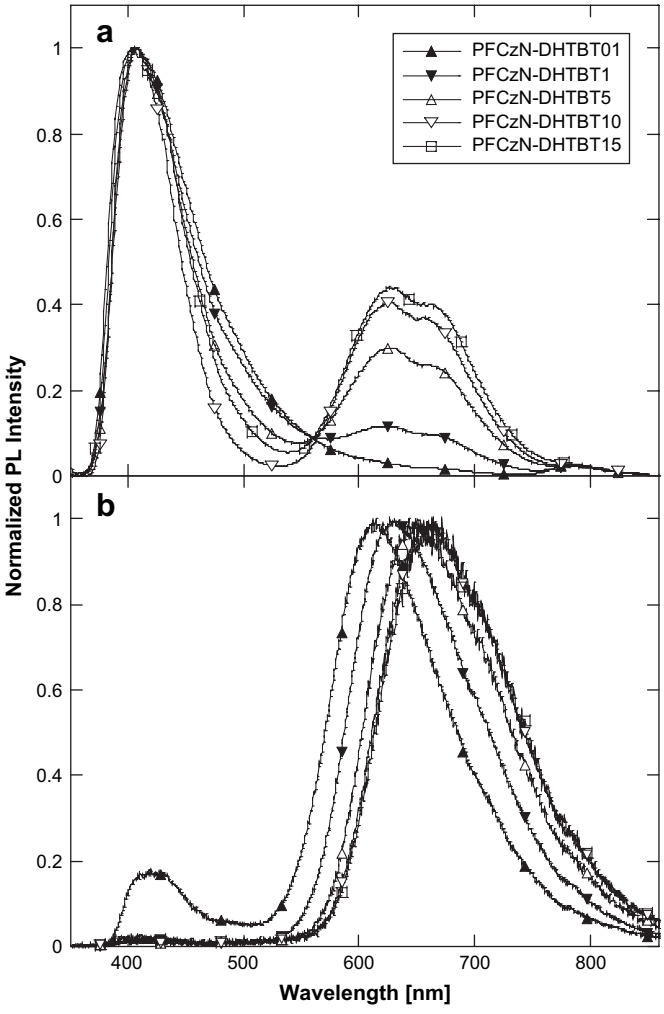

Fig. 3. PL spectra for the polymers: (a) in $CHCl_3$ solution (10^{-5} mol/L) and (b) in film.

4.4. Electroluminescent properties

Owing to the low electron affinity and low drifting mobility of electron in EL polymers, the electron injection between the emitting layer and the metal cathode should be improved to obtain a more balanced charge carriers in the device. Low work functional metals, such as Ba (work function $\varphi = 2.8$ eV) and Ca ($\varphi = 2.9$ eV), are typically used as cathodes to facilitate the electron injection. Since low work functional metals are susceptible to degradation upon exposure to water and oxygen, more stable electron injection cathodes made of high work functional metals are desirable. The PFCzN–DHTBT copolymer can function as both light-emitting and electron injection layers simultaneously. The EL spectra of these copolymers are presented in Fig. 4. It is shown that only a red emission is observed even though the DHTBT content is as low as 0.1 mol%. This fact indicates that energy transfer in EL process from FCzN segment to DHTBT unit is efficient and complete, as like the case of PL emission. The quenched host emission at DHTBT content as low as 1 mol% for both PL and EL processes implies that the

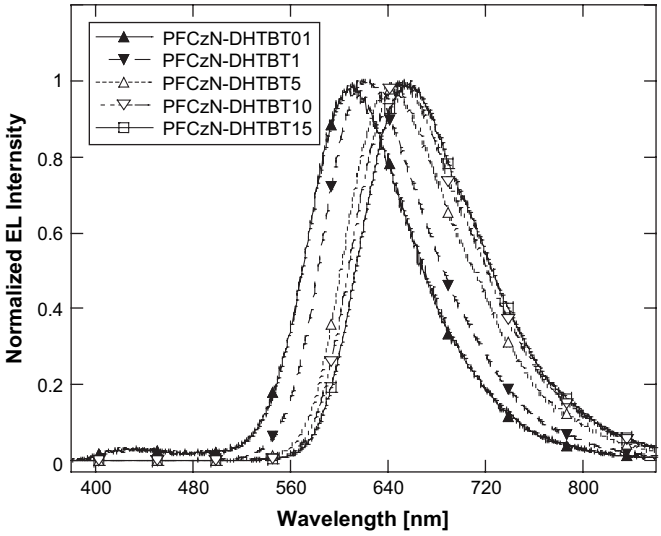

Fig. 4. EL spectra of the devices based on the polymers.

Table 3
Device performances of the polymers with PEDOT as an anode buffer

Polymer	Anode buffer	Cathode	Bias (V)	L_{max} (cd/m^2)	EQE_{max} (%)	$\lambda_{EL,\ max}$ (nm)	CIE coordinates	
							x	*y*
PFCzN–DHTBT01	PEDOT	Ba/Al	9.4	338	0.39	614	0.58	0.40
		Al	11.1	81	0.11			
PFCzN–DHTBT1	PEDOT	Ba/Al	14.4	430	0.22	625	0.63	0.37
		Al	14.9	154	0.15			
PFCzN–DHTBT5	PEDOT	Ba/Al	6.4	243	0.55	643	0.65	0.34
		Al	8.8	165	0.32			
PFCzN–DHTBT10	PEDOT	Ba/Al	5.0	484	0.59	652	0.67	0.33
		Al	6.6	408	0.28			
PFCzN–DHTBT15	PEDOT	Ba/Al	6.7	410	0.57	658	0.68	0.32
		Al	9.2	387	0.30			

energy transfer of PFCzN–DHTBT copolymers occurs mainly via trapping mechanism. The generated exciton is efficiently confined on the DHTBT site, so that polymers emit exclusively the narrow-band-gap component DHTBT. EL peaks are generally 20 nm red-shifted (Tables 2 and 3) in comparison with the PL emission of corresponding copolymers. The red-shifted EL emission with the increasing DHTBT content, as observed in PL spectra, from 614 nm for PFCzN–DHTBT01 to 658 nm for PFCzN–DHTBT15, indicates an aggregation among DHTBT units of neighboring chains.

The EL performances of polymers were examined in the device configuration of ITO/PEDOT (or PVK)/polymer/(or Ba)/Al. The detailed device performances are listed in Tables 3 and 4. It is shown that all polymers show similar external quantum efficiencies, regardless of whether a low functional metal Ba or a high functional metal Al was used as the cathode. The maximum external quantum efficiencies (EQE_{max})s of devices with Al as cathode and PVK as anode buffer layer for PFCzN–DHTBT01, PFCzN–DHTBT1, PFCzN–DHTBT5, PFCzN–DHTBT10 and PFCzN–DHTBT15 are 0.18%, 0.23%, 0.75%, 0.84% and 0.77%, respectively (Table 4). The (EQE_{max})s for PFCzN–DHTBT10 are 1.10% and 0.84% at the luminance of 624 and 507 cd/m^2, respectively, with device configuration: ITO/PEDOT/PVK/polymer/(or Ba)/Al.

The comparable device efficiencies achieved by Al and Ba cathodes for copolymers in this paper indicate that the barrier height on the interface between the active layer and Al cathode is significantly reduced to allow efficient electron injection [36]. Tables 3 and 4 compare the device performances of polymers using PEDOT–PSS or PVK as anode buffer. It can be found that the device efficiencies are significantly enhanced for all copolymers except PFCzN–DHTBT01 and PFCzN–DHTBT1 when PVK was used as anode buffer. Since HOMO and LUMO levels for the copolymer are around −5.2 and −3.1 eV (Table 2), while the work functions of PEDOT and Ba are around 5.0–5.2 eV and 2.8 eV, respectively, obviously there exists no injection barrier for electron, while there is a barrier of 0.2 eV for hole to overcome. The current densities (J) and luminances (L) of the devices versus voltage (V) of the device of PFCzN–DHTBT10 copolymer with different configurations are shown in Fig. 5. It is noticeable that the devices with Al cathode show almost the same operating voltage as the devices with Ba/Al cathode. Moreover, as shown in Fig. 5, the decreased current densities of the devices with PVK buffer layer compared with PEDOT devices indicate that the electron leakage current is depressed leading to an enhanced efficiency. Therefore, it suggests that PVK (HOMO: −5.4 eV, LUMO: −1.9 eV) [37] plays a role of

Table 4
Device performances of the polymers with PVK as an anode buffer

Polymer	Anode buffer	Cathode	Bias (V)	L_{max} (cd/m^2)	EQE_{max} (%)	$\lambda_{EL,\ max}$ (nm)	CIE coordinates	
							x	*y*
PFCzN–DHTBT01	PVK	Ba/Al	16	184	0.30	614	0.58	0.40
		Al	22	83	0.18			
PFCzN–DHTBT1	PVK	Ba/Al	23	203	0.30	625	0.63	0.37
		Al	22	197	0.23			
PFCzN–DHTBT5	PVK	Ba/Al	13	197	0.72	643	0.65	0.34
		Al	12	197	0.75			
PFCzN–DHTBT10	PVK	Ba/Al	10	624	1.10	652	0.67	0.33
		Al	11	507	0.84			
PFCzN–DHTBT15	PVK	Ba/Al	10	489	1.00	658	0.68	0.32
		Al	11	470	0.77			

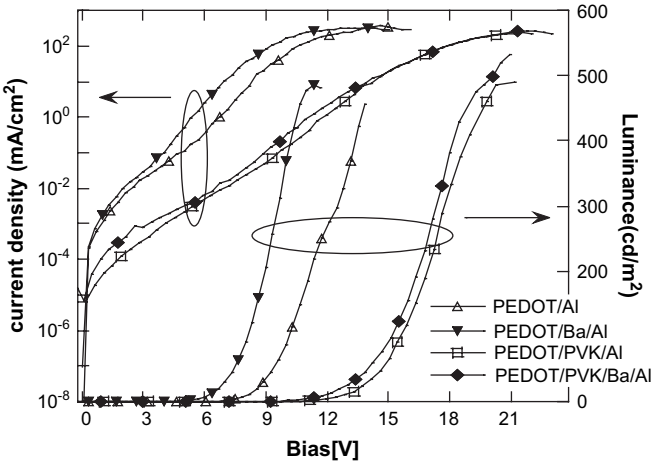

Fig. 5. Current densities (J) and luminances (L) of the devices versus voltage (V) characteristics of the device of PFCzN–DHTBT10 copolymer with different configurations.

electron-blocking and leads to more balanced charge carriers in the device.

5. Conclusions

Amino-containing saturated red light-emitting copolymers PFCzN–DHTBT were synthesized via Suzuki polycondensation. The dimethylaminopropyl group in the polymer side chain can lower the barrier height on the interface between metal cathode and light-emitting polymer. As a result, high work functional metal Al can be used as cathode in PLEDs with similar device performances to those with lower work functional metal Ba cathode. The (EQE_{max})s of the copolymer PFCzN–DHTBT10 achieved 0.84% (or 1.1%) with the device configuration: ITO/PEDOT/PVK/polymer/Al (or Ba/Al) with an emission peaked at 650 nm.

Acknowledgement

The authors are grateful to the Ministry of Science and Technology (No. 2002CB 613402), and the National Natural Science Foundation of China (No. 20574021, U0634003, 50433030) for their financial support.

References

[1] Burroughes JH, Bradley DDC, Brown AR, Marks RN, Mackay K, Friend RH, et al. Nature 1990;347:539.
[2] Hide F, Diaz-Garcia MA, Schwartz BJ, Heeger AJ. Acc Chem Res 1997;30:430.
[3] Friend RH, Gymer RW, Holmes AB, Burroughes JH, Marks RN, Taliani C, et al. Nature 1999;397:121.
[4] Burroows PE, Gu G, Bulovic V, Shen Z, Forrest SR, Thompson ME. IEEE Trans Electron Devices 1997;44:1188.
[5] Scherf U, List EJW. Adv Mater 2002;14:477.
[6] Redecker M, Bradley DDC, Inbasekaran M, Wu WW, Woo EP. Adv Mater 1999;11:241.
[7] Schmitt C, Nothofer HG, Falcou A, Scerf U. Macromol Rapid Commun 2001;22:624.
[8] Kreyenschmidt M, Klaerner G, Fuhrer T, Ashenhurst J, Karg S, Chen WD, et al. Macromolecules 1998;31:1099.
[9] Lee JIG, Daver MH, Miller RD. Synth Met 1999;102:1087.
[10] Liu B, Yu WL, Lai YH, Huang W. Macromolecules 2000;33:8945.
[11] Sung HH, Lin HC. Macromolecules 2004;37:7945.
[12] Wu CW, Lin HC. Macromolecules 2006;39:7232.
[13] Woo EP, Inbasekaran M, Shiang W, Roof GR. WO 9905184; 1997.
[14] Beaupre S, Leclerc M. Adv Funct Mater 2002;12:192.
[15] Drolet N, Beaupre S, Morin JF, Tao Y, Leclerc MJ, Opt A. Pure Appl Opt 2002;4:S252.
[16] Charas A, Morgado J, Martinho JMG, Alcácer L, Cacialli F. Synth Met 2002;127:215.
[17] Yang J, Jiang CY, Zhang Y, Yang RQ, Yang W, Hou Q, et al. Macromolecules 2004;37:1211.
[18] Jenekhe SA, Osaheni JA. Science 1994;265:765.
[19] Chen ZK, Meng H, Lai YH, Huang W. Macromolecules 1999;32:4351.
[20] Huang F, Hou LT, Wu HB, Wang XH, Shen HL, Cao W, et al. J Am Chem Soc 2004;126:9845.
[21] Wu HB, Huang F, Mo YQ, Yang W, Wang DL, Peng JB, et al. Adv Mater 2004;16:1826.
[22] Leclerc M. J Polym Sci Part A Polym Chem 2001;22:1365.
[23] Grice AW, Bradeley DDC, Bernius MT, Inbasekaran M, Wu WW, Woo EP. Appl Phys Lett 1998;73:629.
[24] Bernius MT, Inbasekaran M, Brien JO, Wu W. Adv Mater 2000;13:1737.
[25] Bernius MT, Inbasekaran M, Woo E, Wu WS, Wujkowski L. J Mater Sci Mater Electron 2000;111:11.
[26] Millard IS. Synth Met 2000;119:112.
[27] Pschirer NG, Bunz UHF. Macromolecules 2000;33:3961.
[28] Ranger M, Rondeau D, Leclerc M. Macromolecules 1997;30:7686.
[29] Hou Q, Xu YS, Yang W, Yuan M, Peng JB, Cao Y. J Mater Chem 2002;12:2887.
[30] Hou Q, Zhou QM, Zhang Y, Yang W, Yang RQ, Cao Y. Macromolecules 2004;37:6299.
[31] Kitamura C, Tanaka S, Yamashita Y. Chem Mater 1996;8:570.
[32] Liu CH, Chen SH, Chen Y. J Polym Sci Part A Polym Chem 2006;44:3882.
[33] Yang W, Hou Q, Liu CZ, Niu YH, Huang J, Yang RQ, et al. J Mater Chem 2003;13:1351.
[34] Bredas JL, Silbey R, Boudreaux DS, Chance RR. J Am Chem Soc 1983;105:6555.
[35] Cao Y, Yu G, Zhang C, Menon R, Heeger AJ. Synth Met 1997;87:171.
[36] Huang F, Hou LT, Shen HL, Jiang JX, Wang F, Zhen HY, et al. J Mater Chem 2005;15:2499.
[37] Chen FC, Chang SC, He GF, Pyo S, Yang Y, Kurotaki MY, et al. J Polym Sci B 2003;41:2681.